



Article

Lipoic Acid Gold Nanoparticles Functionalized with Organic Compounds as Bioactive Materials

Ioana Turcu ¹, Irina Zarafu ¹, Marcela Popa ^{2,3}, Mariana Carmen Chifiriuc ^{2,3}, Coralia Bleotu ^{2,4}, Daniela Culita ⁵, Corneliu Ghica ⁶ and Petre Ionita ^{1,5,*}

¹ Department of Organic Chemistry, Biochemistry and Catalysis, University of Bucharest, 90-92 Panduri, 050663 Bucharest, Romania; oana_turcu@yahoo.com (I.T.); zarafuirina@yahoo.fr (I.Z.)

² Microbiology Department, Faculty of Biology, University of Bucharest, 1-3 Portocalelor Way, 060101 Bucharest, Romania; bmarcelica@yahoo.com (M.P.); carmen_balotescu@yahoo.com (M.C.C.); cbleotu@yahoo.com (C.B.)

³ Research Institute of the University of Bucharest-ICUB, 91-95 Spl. Independentei, 050095 Bucharest, Romania

⁴ Romanian Academy, Ștefan S. Nicolau Institute of Virology—IVN, 285 Mihai Bravu Avenue, Sector 3, PO 77, PO Box 201, 030304 Bucharest, Romania

⁵ Institute of Physical Chemistry, 202 Spl. Independentei, 060021 Bucharest, Romania; danaculita@yahoo.co.uk

⁶ National Institute of Materials Physics, Laboratory of Atomic Structures and Defects in Advanced Materials, Atomistilor 105 bis, 077125 Magurele, Romania; cghica@infim.ro

* Correspondence: p_ionita@yahoo.co.uk; Tel.: +40-213051435

Academic Editor: Thomas Nann

Received: 12 December 2016; Accepted: 7 February 2017; Published: 16 February 2017

Abstract: Water soluble gold nanoparticles protected by lipoic acid were obtained and further functionalized by standard coupling reaction with 1-naphtylamine, 4-aminoantipyrine, and 4'-aminobenzo-15-crown-5 ether. Derivatives of lipoic acid with 1-naphtylamine, 4-aminoantipyrine, and 4'-aminobenzo-15-crown-5 ether were also obtained and characterized. All these were tested for their antimicrobial activity, as well as for their influence on mammalian cell viability and cellular cycle. In all cases a decreased antimicrobial activity of the obtained bioactive nanoparticles was observed as compared with the organic compounds, proving that a possible inactivation of the bioactive groups could occur during functionalization. However, both the gold nanoparticles as well as the functionalized bioactive nanosystems proved to be biocompatible at concentrations lower than 50 µg/mL, as revealed by the cellular viability and cell cycle assay, demonstrating their potential for the development of novel antimicrobial agents.

Keywords: gold nanoparticles; lipoic acid; thioctic acid; antimicrobial; cytotoxicity; cellular cycle

1. Introduction

Gold has been used for therapeutic purposes since ancient times, being mentioned in Chinese medical history in 2500 BC, still used in colloidal form in the Indian Ayurveda, and also used in western medicine for a wide range of muco-cutaneous, connective, and nervous tissues disorders [1,2].

Gold nanoparticles (Au NPs) are increasingly exploited for the design and development of novel nanomedicines, due to their ease of synthesis, characterization, and surface functionalization [3]. Different studies demonstrate their excellent antimicrobial properties, with a large spectrum including *Gram-positive* and *Gram-negative* bacteria, including multidrug resistant strains [4–6], as well as antiretroviral activity [7]. Functionalized gold nanoparticles have also been shown to increase the activity of antibiotics (e.g., *Vancomycin* against resistant enterococci, aminoglycosides) [8,9] or to act synergically (e.g., with *Cefaclor*, a second-generation β-lactam antibiotic, probably by targeting multiple bacterial targets, such as creating holes in the bacterial murein wall and/or interfering with the DNA

condensation) [10]. However, in order to achieve the translation into clinical practice as novel tools for the antimicrobial therapy, much research is needed in order to elucidate the intimate mechanisms of action and interaction with target molecular structures, as well as the related acute and chronic toxicity issues.

Biomolecules bound on the surface of nanoparticles can simultaneously play several essential roles, like preserving the size of the main core, acting as a stabilizing ligand, and making further functionalization steps possible [11–14].

Gold nanoparticles have the advantage of versatility [15] and are commonly used for labeling with various organic compounds, and therefore can be employed as vectors containing the attached organic compounds with their desired properties. Moreover, Au NPs have unique advantages in DNA or RNA delivery to mammalian cells [16–19].

One kind of chemical reaction is based on the affinity of gold for thiol groups [9]. For example, lipoic acid (LA) is a disulfide that is well known as an antioxidant and it is reduced at intra-cellular levels into dihydrolipoic acid, a dithiol which has strong antioxidant properties [20]. In medicine it is used in many diseases, due to its antioxidant activity. Some *in vivo* and *in vitro* studies report that LA is very useful in the treatment of hyperglycemia or diabetes [21], due to its capability to stimulate the uptake of glucose into the muscle cells, where glucose is consumed.

In our study, we obtained water soluble gold nanoparticles protected by lipoic acid; these kinds of Au NPs are also known in the literature [22]. Using a standard coupling reaction of the carboxyl groups from the Au NPs with the amino groups from 4-aminoantipyrine, 4'-aminobenzo-15-crown-5 ether, and 1-naphthylamine, we obtained functionalized Au NPs and evaluated their possible biological activities, by the *in vitro* study of their interaction with microbial and mammalian cells.

2. Materials and Methods

2.1. Materials and Apparatus

All chemicals and solvents were purchased from Aldrich (Bucharest, Romania) or Chimopar (Bucharest, Romania). ^1H - and ^{13}C -NMR spectra were recorded on a Bruker 300 MHz instrument (Rheinstetten, Germany), using deuterated chloroform as the solvent and tetramethylsilane (TMS) as the internal standard. Infrared (IR) spectra were recorded on a Bruker FT-IR apparatus (Bremen, Germany). UV-Vis spectra were recorded in water at room temperature using an UVD-3500 double beam spectrophotometer (Labomed, LA, USA). Dynamic light scattering (DLS) analysis was performed in water on a Beckman Coulter particle size analyzer (Brea, CA, USA) using the Delsa Nano software (Beckman Coulter, Brea, CA, USA). Transmission electron microscopy (TEM) pictures were obtained using a Jeol 200 CX microscope (Jeol, Tokyo, Japan); a drop of diluted Au NPs was added on a 3 mm carbon copper grid and left to dry.

2.2. Synthesis of Gold Nanoparticles

LA Au NPs were obtained by dissolving 50 mg of hydrogen tetrachloroaurate into 50 mL of methanol, and under stirring a solution which was prepared by dissolving 50 mg of LA into 50 mL of methanol was added. After about 10 min, 50 mg of sodium borohydride dissolved in 5 mL of water was added to the mixture. The colour of the mixture turned from opalescent yellow-orange to black, while some hydrogen gas also evolved. After one hour, the mixture was left to settle; a black precipitate appears and this was separated by decantation of the liquid and by washing three times with methanol. For purification, the separated solid was dissolved in water and dialyzed for 24 h (diluted ammonia solution may be required in order to increase the solubility of the precipitate). The resulting purified LA Au NPs can be stored as a water solution, at $\text{pH} \approx 9$ (by adding small amounts of sodium hydroxide or ammonia).

2.3. Functionalization of Gold Nanoparticles

As a general procedure, to 2 mL of dialyzed LA Au NPs, 20 mg of the corresponding amine (4-amino-antipyrine, 4-amino-benzo-15-crown-5 or 1-naphtylamine) was added which was dissolved before in 2 mL of isopropyl alcohol and 20 mg of 1-ethyl-3-(3-dimethyl aminopropyl)carbodiimide hydrochloride (EDC). The resulting mixture was left under stirring for three days and was then dialyzed for 1 day against 1000 mL of deionised water.

2.4. Synthesis of the Compounds V–VII

General procedure: To 1 mmol LA dissolved into 50 mL DCM, 1 mmol of the corresponding amine and 1.2 mmol of EDC hydrochloride was added and the mixture was stirred for three days. The solution was then extracted once with diluted aqueous hydrochloric acid (1 M) and once with diluted sodium hydrogen carbonate, and then the organic phase was dried over anhydrous sodium sulfate, filtered off, and the solvent was removed. The crude product was purified by column chromatography using silica as the stationary phase and ethyl acetate as the eluent. The yield was about 30%.

Compound V: $^1\text{H-NMR}$ (CDCl_3 , ppm): 7.88–7.44 (m, 7H, *naphtyl*); 3.67–3.54 (t, 1H, S-CH); 3.18–3.10 (m, 2H, S-CH₂); 2.54–2.39 (m, 2H, CH₂); 2.32 (t, 2H, CH₂-CO); 1.93–1.50 (m, 6H, CH₂). $^{13}\text{C-NMR}$ (CDCl_3 , ppm): 177.56; 157.09; 154.01; 128.74; 126.29; 125.89; 125.70; 121.24; 120.67; 56.39; 40.22; 38.46; 34.66; 33.81; 28.81; 24.80. IR (cm^{-1}): 3320; 2927; 2850; 1625; 1531; 1448; 1242; 1087; 772; 640; 417.

Compound VI: $^1\text{H-NMR}$ (CDCl_3 , ppm): 8.29 (s, 1H, NH); 7.50–7.32 (m, 5H, *phenyl*); 3.61–3.57 (m, 1H, S-CH); 3.56–3.12 (m, 2H, S-CH₂); 3.10 (s, 3H, N-CH₃); 2.49–2.45 (m, 2H, CH₂); 2.34 (t, 2H, CH₂-CO); 2.25 (s, 3H, C-CH₃); 1.96–1.90 (m, 2H, CH₂); 1.83–1.68 (m, 2H, CH₂); 1.49–1.46 (m, 2H, CH₂). $^{13}\text{C-NMR}$ (CDCl_3 , ppm): 172.28; 161.76; 149.62; 134.47; 129.29; 127.10; 124.46; 108.71; 56.41; 40.20; 38.46; 36.03; 35.86; 34.66; 28.81; 25.31; 12.47. IR (cm^{-1}): 3238; 3034; 2926; 2851; 1684; 1644; 1619; 1591; 1295; 759; 695; 589.

Compound VII: $^1\text{H-NMR}$ (CDCl_3 , ppm): 8.16 (s, 1H, NH); 7.35 (s, 1H, CH_{phenyl}); 6.97 (d, 1H, CH_{phenyl}); 6.72 (d, 1H, CH_{phenyl}); 4.05 (s, 4H, CH₂-O); 3.86–3.82 (d, 4H, CH₂-O); 3.72 (s, 8H, CH₂-O); 3.58–3.54 (t, 1H, S-CH); 3.17–3.07 (m, 2H, S-CH₂); 2.45–2.38 (m, 2H, CH₂); 2.40 (t, 2H, CH₂-CO); 1.93–1.88 (m, 2H, CH₂); 1.72–1.68 (m, 2H, CH₂); 1.49–1.47 (m, 2H, CH₂). $^{13}\text{C-NMR}$ (CDCl_3 , ppm): 171.81; 148.68; 145.16; 132.33; 114.39; 112.84; 107.11; 70.95–68.34; 56.39; 53.41; 40.21; 38.45; 36.80; 34.60; 28.81; 25.41. IR (cm^{-1}): 3324; 2926; 2850; 1626; 1560; 1308; 1241; 1086; 891; 640; 416.

2.5. Biological Activity

The antimicrobial assays were performed on the following reference strains, i.e., Gram-positive (*Staphylococcus aureus* ATCC 6538, *Bacillus subtilis* ATCC 6633, *Enterococcus faecalis*) and Gram-negative (*Escherichia coli* ATCC 8739, *Pseudomonas aeruginosa* ATCC 9027) bacteria and the fungus *Candida albicans* ATCC 10231. The quantitative assay of the antimicrobial activity was performed by the liquid medium microdilution method, in 96 multi-well plates, in order to establish the minimal inhibitory concentration (MIC). For this purpose, serial two-fold dilutions of the compounds ranging between 1000 and $1.95 \mu\text{g}\cdot\text{mL}^{-1}$ were performed in a 200 μL volume of broth and each well was seeded with 50 μL microbial inoculum. Sterility controls (wells containing only culture medium) and culture controls (wells containing culture medium seeded with the microbial inoculum) were used. The plates were incubated for 24 h at 37 °C, and MIC values were considered as the lowest concentration of the tested compound that inhibited the visible growth of the microbial overnight cultures [23–28].

For the cellular viability assay, a HeLa cell line was seeded into 96-well plates at 5×10^3 cells/well. After 24 h, binary dilutions of each compound (100, 50, and 25 $\mu\text{g}/\text{mL}$) were added and the cells were maintained for another 24 h at 37 °C, 5% CO₂, in a humid atmosphere. The cell viability was evaluated using the CellTiter 96[®] Aqueous One Solution Cell Proliferation Assay (Promega Dexter Com S.R.L.,

Bucharest, Romania) measuring the absorbance at 490 nm in an enzyme-linked immunosorbent assay (ELISA) reader.

For the cell cycle assay, monolayers of HeLa cells were cultivated in RPMI 1640 (Gibco) supplemented with 10% heat-inactivated bovine serum and penicillin/streptomycin at 37 °C with 5% CO₂. The 24 h monolayers were treated with two different concentrations (100 and 50 µg/mL) of the stock suspension of the tested nanoparticles. After that, they were maintained for another 24 h at 37 °C, in 5% CO₂ in a humid atmosphere. After the incubation time, the cells were harvested, washed with PBS (pH 7.5), fixed in 70% cold ethanol, and maintained overnight at −20 °C. Each sample was washed in PBS, treated with 100 µg/mL RNase A (1 mg/mL), and stained with 10 µg/mL propidium iodide (PI) by incubation at 37 °C for 1 h. After PI staining of the cells, the events acquisition was performed using an Epics Beckman Coulter flow cytometer (SKU, Ramsey, MN, USA). The cytotoxicity of the tested nanoparticles was assessed by a colorimetric method using the tetrazolium salt [3-(4,5-dimethyl-2-yl)-5-(3-carboxymethoxyphenyl)-2-(4-sulfophenyl)-2H-tetrazolium; MTS] and using phenazine ethosulfate as an electron coupling reagent which forms a stable solution with MTS. The MTS tetrazolium compound is bio-reduced by nicotinamide adenine dinucleotide phosphate (NADPH or NADH) dehydrogenase enzymes in metabolically active cells into a colored formazan product that is soluble in the tissue culture medium. Therefore, the value of the absorbance of the treated cells' culture medium recorded at 490 nm is directly proportional with the percentage of viable cells. The obtained data were analyzed using FlowJo 8.8.6 software (Ashland, OR, USA).

3. Results and Discussion

3.1. Synthesis of Gold Nanoparticles

Water soluble Au NPs can be easily obtained by the reduction of gold ions with sodium borohydride in the presence of LA; while disulphide groups are attached to the gold surface, thus stabilizing the nanoparticles, the free carboxylic acid groups make possible their dispersion in water (Figure 1, left); fully coated Au NPs with an average size of 16 nm are obtained in this way (namely sample I), as shown by the dynamic light scattering (DLS) analysis (see Supplementary Information (SI), Figure S1). Transmission electron microscopy (TEM) analysis of the LA protected Au NPs showed an average size of about 10 nm (Figure 1, right), with a large polydispersity. It is also well known that DLS analysis give the hydrodynamic diameter of the Au NPs, not the actual diameter. Also, the ultraviolet and visible (UV-Vis) spectrum showed the expected plasmon resonance band at about 510 nm (SI, Figure S2), while the IR spectrum of the LA functionalized Au NPs showed the presence of the carboxylic groups at about 1650 cm^{−1} (a very broad band can also be noticed between 3000–3500 cm^{−1}, see SI Figure S3).

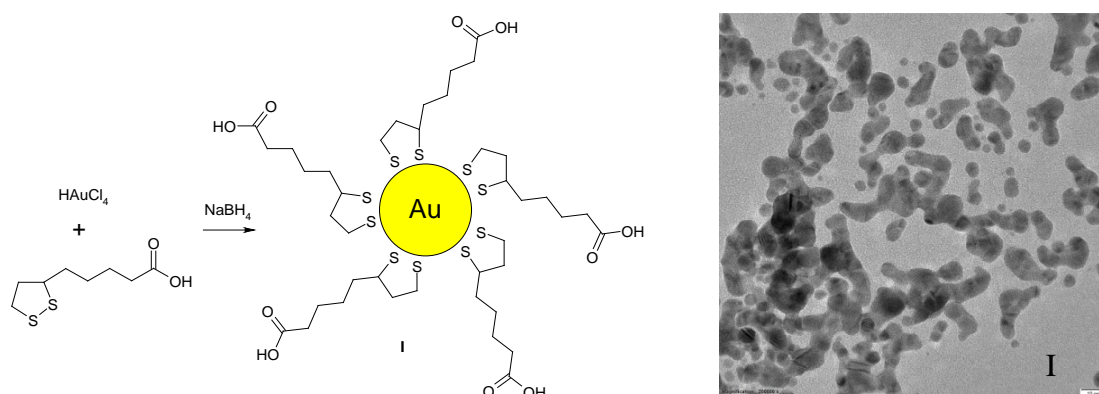


Figure 1. Synthesis of lipoic acid (LA) Au NPs (left) and their transmission electron microscopy (TEM) image (right). Scale bar 10 nm.

3.2. Functionalization of Gold Nanoparticles

The functionalization of such Au NPs is easily performed using standard organic chemistry. Starting from LA Au NPs and using the coupling reaction in the presence of EDC between the COOH group from LA and the NH₂ group from the amine (naphthylamine, amino-antipyrine, and amino-benzo-15-crown-5, Figure 2, top) it was possible to obtain Au NPs that are derivatized with the desired compounds (samples II–IV, Figure 2). These are easily purified by dialysis, as the un-reacted amines and the coupling agent pass freely through the dialysis membrane, while the Au NPs do not. These nanoparticles were also characterized by UV-Vis and IR spectroscopy. UV-Vis spectra showed that the plasmon bands were bathochromic shifted by about 10 nm, due to the functionalization of the Au NPs (SI, Figure S4).

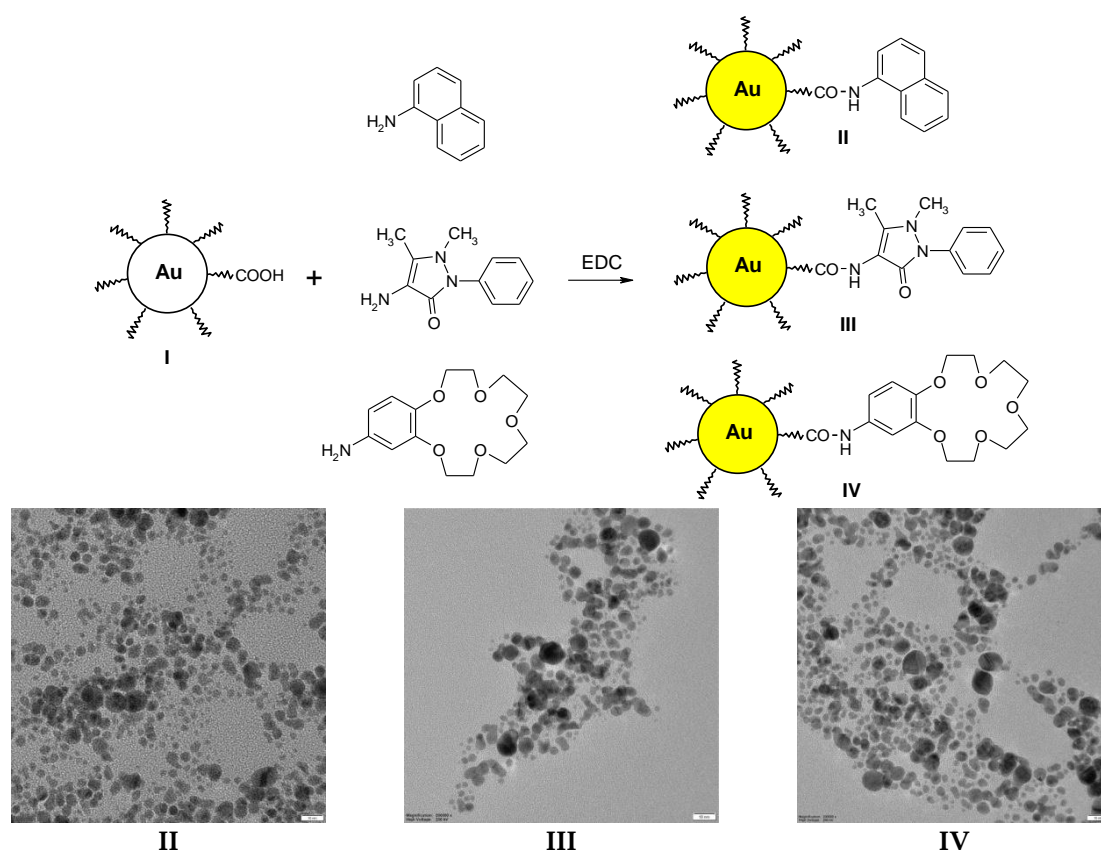


Figure 2. Top: Functionalization of Au NPs (I) with 1-naphthylamine, 4-aminoantipyrine, and 4'-amino-benzo-crown-5, yielding samples II–IV; Bottom: TEM images of samples II, III, and IV, respectively (scale bar 10 nm).

The IR spectra of the same samples showed the presence of a strong band at 1626 cm^{-1} and a smaller band at 1685 cm^{-1} , assigned to the new amidic bonds formed during the functionalization reactions (SI, Figure S5); moreover, the broad band which appeared before in the LA Au NPs between $3000\text{--}3500\text{ cm}^{-1}$ disappeared, while three new sharp bands emerged at 2850 , 2930 , and 3325 cm^{-1} . These are due to the replacement of the carboxyl groups with the amide groups corresponding to the naphthylamine, amino-antipyrine, and amino-benzo-15-crown-5 derivatives. All these data confirm the functionalization of the starting LA Au NPs.

In addition, the DLS measurements of the functionalized samples showed an increase in the size of the nanoparticles (average size of 66 nm for 1-naphthylamine, 48 nm for 4-aminoantipyrine, and 86 nm for 4'-amino-benzo-crown-5, SI Figure S6a–c), meaning that some agglomeration of the Au NPs occurs during functionalization. The TEM analysis showed similar behavior as the starting LA

protected Au NPs; however, the nanoparticles are better dispersed (Figure 2, bottom). Additional TEM pictures are shown in SI, Figure S7.

3.3. Synthesis of the Compounds V–VII

In order to compare the biological activity of the labelled Au NPs with their organic ligand, we synthesised compounds V–VII (Figure 3) following similar coupling reactions. Although these compounds are known in the literature [29], they were characterized by $^1\text{H-NMR}$, $^{13}\text{C-NMR}$, and IR, thus confirming their structure (see Methods and Materials for details).

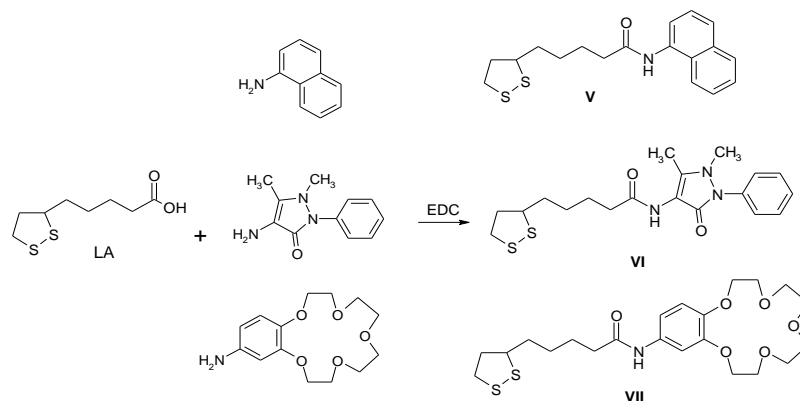


Figure 3. Synthesis of the compounds V–VII starting from LA.

3.4. Biological Activity

The bare gold nanoparticles (sample I), as well as those functionalized with 1-naphthylamine (compound V), exhibited a low antimicrobial activity against all the tested microbial strains, with MIC values higher than 1 mg/mL (Table 1). Moreover, compound V exhibited a higher antimicrobial activity against *B. subtilis* (MIC of 0.25 $\mu\text{g}/\text{mL}$) than that exhibited by the resulting functionalized nanoparticles, demonstrating a possible inactivation of the bioactive groups during functionalization.

Table 1. Minimal inhibitory concentration (MIC) values of the tested compounds against the tested microbial strains.

Sample	<i>E. coli</i>	<i>P. aeruginosa</i>	<i>E. faecalis</i>	<i>S. aureus</i>	<i>B. subtilis</i>	<i>C. albicans</i>
I	>1	>1	>1	>1	>1	>1
II	>1	>1	>1	>1	1	>1
III	>1	>1	>1	>1	>1	>1
IV	>1	>1	>1	>1	>1	>1
V	>1	>1	>1	>1	0.25	>1
VI	>1	0.031	1	>1	0.002	>1
VII	>1	0.004	>1	>1	1	>1

Compound VI proved to be the most active from the tested series, exhibiting a very good antimicrobial activity against *P. aeruginosa* (MIC of 0.031 mg/mL) and *B. subtilis* (MIC of 0.002 mg/mL) (Table 1). The antimicrobial activity of the functionalized nanoparticles with amino-antipyridine was also lower than that of the components, i.e., gold nanoparticles I and compound VI, probably due to the inactivation of the active groups during functionalization. The gold nanoparticles functionalized with the crown ether (sample IV) exhibited a very low antimicrobial activity. It is to be noticed that compound VII exhibited a very low MIC value against the *P. aeruginosa* strain (0.004 mg/mL), but this inhibitory effect was not observed after functionalization. The low activity can be due to the loss of the carboxyl and amino groups by functionalization.

Moreover, the very low activity noticed for samples II–IV compared with V–VII can be attributed also to the low organic content in the Au NP samples. These organic functionalized nanoparticles are composed of a ‘heavy’ Au metallic core protected by a ‘light’ single layer or thiol derivative. In the case of sample I, the thiol derivative is LA (Au NPs are practically protected by LA); for samples II–IV, only some LA from the Au NPs’ surface are functionalized by naphthyl, crown ether, or antipyrine moieties, as the EDC coupling reaction is not quantitative.

Regarding the cytotoxic assay, the tested nanoparticles exhibited different levels of cytotoxicity, depending on the type and tested concentration. Compounds V and VII proved to be the most cytotoxic at the higher tested concentrations of 100 and 50 $\mu\text{g}/\text{mL}$. The gold nanoparticles (I) proved to not be cytotoxic to HeLa cells, irrespective of the tested concentration. The rest of the tested nanoparticles exhibited low degrees of cytotoxicity, with this effect being observed only at the highest tested concentration of 100 $\mu\text{g}/\text{mL}$, and were not cytotoxic at the two lower tested concentrations (Figure 4).

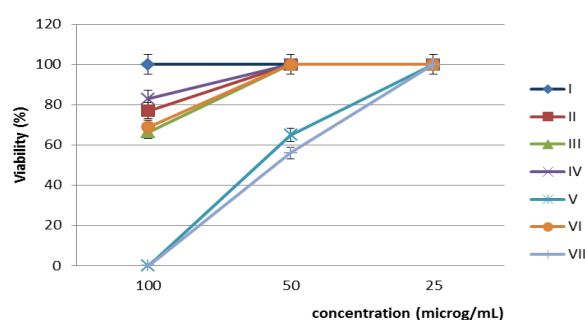


Figure 4. Viability (%) of HeLa cells after 24 h treatment with different concentrations of the obtained nanoparticles.

The cellular cycle assay confirmed the results of the cellular viability assay. Thus, the gold nanoparticles (I) which did not affect the viability of the HeLa cells did not alter the cellular cycle phases either (Figure 4). In exchange, the other tested compounds which induced variable degrees of cytotoxicity in HeLa cells, did also alter the cellular cycle of the HeLa cells, revealed by the occurrence of a left, sub-G0 peak corresponding to cellular apoptosis, accompanied by a decrease of the percentage of cells found in the G1, S, and G2 phases (Figure 5).

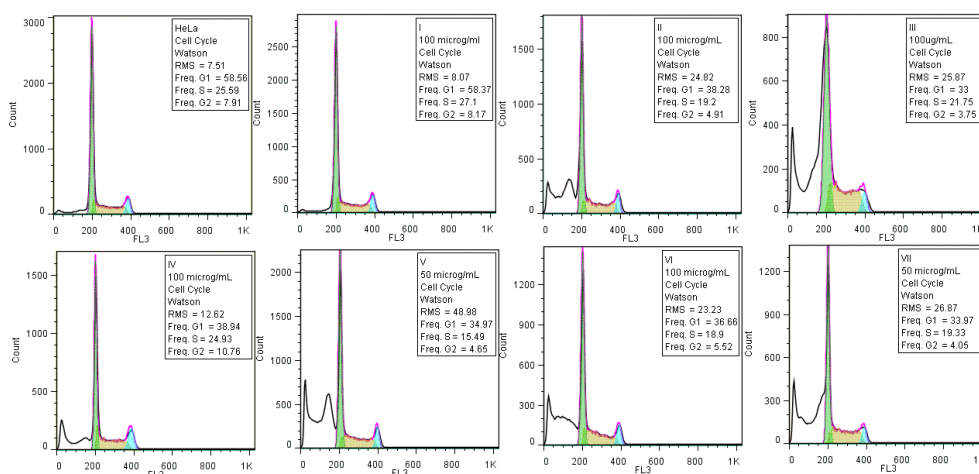


Figure 5. Flow cytometry diagrams of the HeLa cells’ cycle analysis grown in the presence of the tested nanoparticles.

4. Conclusions

Among the obtained nanostructures, the most effective antimicrobial properties were exhibited, in decreasing order, by compounds VI, VII, and V used for the functionalization of gold nanoparticles. In all cases, a decreased antimicrobial activity of the obtained bioactive nanoparticles was observed as compared to the nanosystem components, proving that a possible inactivation of the bioactive groups could occur during functionalization. However, both gold nanoparticles as well as the functionalized bioactive nanosystems proved to be biocompatible at concentrations lower than 50 µg/mL, as revealed by the cellular viability and cell cycle assay, demonstrating their potential for the development of novel antimicrobial agents.

Supplementary Materials: The following are available online at <http://www.mdpi.com/2079-4991/7/2/43/s1>.

Acknowledgments: This work was supported by a grant from the Romanian National Authority for Scientific Research, CNCS – UEFISCDI. Corneliu Ghica acknowledges the financial support from the Core Project PN16-480102.

Author Contributions: Petre Ionita, Ioana Turcu, and Irina Zarafu conceived and designed the experiments; Ioana Turcu, Corneliu Ghica, and Daniela Culita performed the experiments; Mariana Carmen Chifiriuc, Marcela Popa, and Coralia Bleotu performed the biological tests and analyzed the data; Petre Ionita wrote the paper, with contributions and help from all authors.

Conflicts of Interest: The authors declare no conflict of interest.

References

1. Rai, A.; Prabhune, A.; Perry, C.C. Antibiotic mediated synthesis of gold nanoparticles with potent antimicrobial activity and their application in antimicrobial coatings. *J. Mater. Chem.* **2010**, *20*, 6789–6798. [[CrossRef](#)]
2. Felson, D.T.; Anderson, J.J.; Meenan, R.F. The comparative efficacy and toxicity of second-line drugs in rheumatoid arthritis, Results of two meta analyses. *Arthritis Rheumatol.* **1990**, *33*, 1449–1461. [[CrossRef](#)]
3. Arvizo, R.R.; Bhattacharyya, S.; Kudgus, R.; Giri, K.; Bhattacharya, R.; Mukherjee, P. Intrinsic therapeutic applications of noble metal nanoparticles: Past, present and future. *Chem. Soc. Rev.* **2012**, *41*, 2943–2970. [[CrossRef](#)] [[PubMed](#)]
4. Suganya, K.S.; Govindaraju, K.; Kumar, V.G.; Dhas, T.S.; Karthick, V.; Singaravelu, G.; Elanchezhyan, M. Blue green alga mediated synthesis of gold nanoparticles and its antibacterial efficacy against Gram positive organisms. *Mater. Sci. Eng. C* **2015**, *47*, 351–356. [[CrossRef](#)] [[PubMed](#)]
5. Xiaoning, L.; Robinson, S.M.; Gupta, A.; Saha, K.; Jiang, Z.; Moyano, D.F.; Sahar, A.; Riley, M.A.; Vincent, M.R. Functional gold nanoparticles as potent antimicrobial agents against multi-drug-resistant bacteria. *ACS Nano* **2014**, *8*, 10682–10686.
6. Niemirowicz, K.; Swiecicka, I.; Wilczewska, A.Z.; Misztalewska, I.; Kalska-Szostko, B.; Bienias, K.; Bucki, R.; Car, H. Gold-functionalized magnetic nanoparticles restrict growth of *Pseudomonas aeruginosa*. *Int. J. Nanomed.* **2014**, *8*, 2217–2224.
7. Shiang, Y.C.; Ou, C.M.; Chen, S.J.; Ou, T.Y.; Lin, H.J.; Huang, C.C.; Chang, H.T. Highly efficient inhibition of human immunodeficiency virus type 1 reverse transcriptase by aptamers functionalized gold nanoparticles. *Nanoscale* **2013**, *5*, 2756–2764. [[CrossRef](#)] [[PubMed](#)]
8. Grace, N.A.; Pandian, K. Antibacterial efficacy of aminoglycosidic antibiotics protected gold nanoparticles-A brief study. *Int. J. Pharm.* **2007**, *297*, 63–70.
9. Rastogi, L.; Kora, A.J. Highly stable, protein capped gold nanoparticles as effective drug delivery vehicles for amino-glycosidic antibiotics. *Mater. Sci. Eng. C* **2012**, *32*, 1571–1577. [[CrossRef](#)] [[PubMed](#)]
10. Pop, C.S.; Hussien, M.D.; Popa, M.; Mares, A.; Grumezescu, A.M.; Grigore, R.; Lazar, V.; Chifiriuc, M.C.; Sakizlian, M.; Bezirtzoglou, E.; et al. Metallic-based micro and nanostructures with antimicrobial activity. *Curr. Top. Med. Chem.* **2015**, *15*, 1577–1582. [[CrossRef](#)] [[PubMed](#)]
11. Murray, C.B.; Norris, D.J.; Bawendi, M.G. Synthesis and characterization of nearly monodisperse CdE (E = sulfur, selenium, tellurium) semiconductor nanocrystallites. *J. Am. Chem. Soc.* **1993**, *115*, 8706–8715. [[CrossRef](#)]

12. O'Brien, S.; Brus, L.; Murray, C.B. Synthesis of monodisperse nanoparticles of barium titanate: Toward a generalized strategy of oxide nanoparticle synthesis. *J. Am. Chem. Soc.* **2001**, *123*, 12085–12086. [[CrossRef](#)] [[PubMed](#)]
13. Kapoor, S.; Mukherjee, T. Photochemical formation of copper nanoparticles in PVP. *Chem. Phys. Lett.* **2003**, *370*, 83–87. [[CrossRef](#)]
14. Gupta, A.K.; Gupta, M. Synthesis and surface engineering of iron oxide nanoparticles for biomedical applications. *Biomaterials* **2010**, *26*, 3995–4021. [[CrossRef](#)] [[PubMed](#)]
15. Haes, A.J.; Hall, W.P.; Chang, L.; Klein, W.L.; van Duyne, R.P. A localized surface plasmon resonance biosensor; first step towards an assay for Alzheimers disease. *Nano Lett.* **2004**, *4*, 1029–1034. [[CrossRef](#)]
16. Zu, Y.; Huang, S.; Liao, W.; Lu, Y.; Wang, S. Gold nanoparticles enhanced electroporation for mammalian cell transfection. *J. Biomed. Nanotechnol.* **2014**, *10*, 982–992. [[CrossRef](#)] [[PubMed](#)]
17. Guo, S.; Huang, Y.; Jiang, Q.; Sun, Y.; Deng, L.; Liang, Z.; Du, Q.; Zing, J.; Zhao, Y.; Wang, P.C.; et al. Enhanced gene delivery and siRNA silencing by gold nanoparticles coated with charge-reversal polyelectrolyte. *ACS Nano* **2010**, *4*, 5505–5511. [[CrossRef](#)] [[PubMed](#)]
18. Elbakry, A.; Zaky, A.; Liebl, R.; Rachel, R.; Goepferich, A.; Breunig, M. Layer-by-layer assembled gold nanoparticles for siRNA delivery. *Nano Lett.* **2009**, *9*, 2059–2064. [[CrossRef](#)] [[PubMed](#)]
19. Huang, S.; Deshmukh, H.; Rajagopalan, K.; Wang, S. Enhancing electroporation transfection with Au NPs polyplex electrophoresis. *Electrophoresis* **2014**, *35*, 1837–1845. [[CrossRef](#)] [[PubMed](#)]
20. Raschke, G.; Kowarik, S.; Franzl, T.; Sonnichsen, C.; Klar, T.A.; Ferdmann, J. Biomolecular recognition based on single gold nanoparticle light scattering. *Nano Lett.* **2003**, *3*, 935–938. [[CrossRef](#)]
21. Jacob, S.; Streeper, R.S.; Fogt, D.L.; Hokama, J.Y.; Tritschler, H.J.; Dietze, G.J.; Henriksen, E.J. The antioxidant α -lipoic acid enhances insulin-stimulated glucose metabolism in insulin-resistant rat skeletal muscle. *Diabetes* **1996**, *45*, 1024–1029. [[CrossRef](#)] [[PubMed](#)]
22. Roux, S.; Garcia, B.; Bridot, J.-L.; Salomé, M.; Marquette, C.; Lemelle, L.; Gillet, P.; Blum, L.; Perriat, P.; Tillement, O. Synthesis, characterization of dihydrolipoic acid capped gold nanoparticles, and functionalization by the electroluminescent luminol. *Langmuir* **2005**, *21*, 2526–2536. [[CrossRef](#)] [[PubMed](#)]
23. Calu, L.; Badea, M.; Chifiriuc, M.C.; Bleotu, C.; David, G.I.; Ioniță, C.; Măruțescu, L.; Lazăr, V.; Stanică, N.; Soponaru, I.; et al. Synthesis, spectral, thermal, magnetic and biological characterization of Co(II), Ni(II), Cu(II) and Zn(II) complexes with a Schiff base bearing a 1,2,4-triazole pharmacophore. *J. Therm. Anal. Calorim.* **2015**, *120*, 375–386. [[CrossRef](#)]
24. Stecoza, C.E.; Căproiu, M.T.; Drăghici, C.; Chifiriuc, M.C.; Drăcea, N.O. Synthesis, characterization and antimicrobial activity evaluation of some new derivatives of 6,11-dihydrodibenzo[b,e]thiepin 5,5-dioxide. *Rev. Chim.* **2009**, *60*, 137–141.
25. Rosu, T.; Pasculescu, S.; Lazar, V.; Chifiriuc, C.; Cernat, R. Combinations of Cu(II) with mixed ligands derived from 4-amino-2,3-dimethyl-1-phenyl-3-pyrazolin-5-one with biological activity. *Molecules* **2006**, *11*, 904–914. [[CrossRef](#)] [[PubMed](#)]
26. Limban, C.; Balotescu, M.C.; Missir, A.V.; Chiriță, I.C.; Bleotu, C. Antimicrobial activity of some new thiourea derivatives derived from 2-(4-chlorophenoxymethyl)benzoic acid. *Molecules* **2008**, *13*, 567–580. [[CrossRef](#)] [[PubMed](#)]
27. Limban, C.; Marutescu, L.; Chifiriuc, M.C. Synthesis, spectroscopic properties and antipathogenic activity of new thiourea derivatives. *Molecules* **2011**, *16*, 7593–7607. [[CrossRef](#)] [[PubMed](#)]
28. Olar, R.; Badea, M.; Marinescu, D.; Chifiriuc, M.C.; Bleotu, C.; Grecu, M.N.; Iorgulescu, E.; Bucur, M.; Lazar, V.; Finaru, A. Prospects for new antimicrobials based on N,N-dimethylbiguanide complexes as effective agents on both planktonic and adhered microbial strains. *Eur. J. Med. Chem.* **2010**, *45*, 2868–2875. [[CrossRef](#)] [[PubMed](#)]
29. Zhang, S.J.; Ge, Q.F.; Guo, D.W.; Hu, W.X.; Liu, H.Z. Synthesis and anticancer evaluation of alpha-lipoic acid derivatives. *Bioorg. Med. Chem. Lett.* **2010**, *20*, 3078–3083. [[CrossRef](#)] [[PubMed](#)]

